Brajesh Kumar[1],

Yatendra Kumar Singh[1],

Subrat Kumar Swain[2]

Disturbance-Resilient Position Control of Maglev Systems Using Advanced Sliding Mode Techniques

Abstract—Magnetic levitation (maglev) systems exhibit strong nonlinearity and intrinsic instability, making them vulnerable to parameter uncertainties and unforeseen external disturbances, especially in demanding environmental conditions. This paper presents a disturbance observer-based control (DOBC) integrated with a higher-order sliding mode (HOSM) controller to enhance the stability and performance of the maglev system. Traditional sliding mode control (SMC) methods often suffer from high-frequency oscillations, known as chattering, and require precise knowledge of system parameters, which may not always be available. To overcome these challenges, the proposed DOBCbased HOSM controller effectively estimates and compensates for disturbances while ensuring robust position tracking. The controller's performance is evaluated through simulations conducted on a predefined reference trajectory, both in the presence and absence of external disturbances. Comparative analysis with conventional integer-order proportional-integral-derivative (IOPID) and standard HOSM controllers demonstrates the superior disturbance rejection capability and improved tracking accuracy of the proposed approach.

Index Terms—Maglev system, higher order sliding mode (HOSM) control, disturbance observer-based control, Lyapunov stability

1. INTRODUCTION

Maglev systems have gained increasing attention due to their non-contact operation, minimal wear, low noise, and high precision [1], [2]. These advantages make maglev technology suitable for high-speed transportation, space engineering, rocket launch systems, and biomedical instrumentation [2]. However, the highly nonlinear and inherently unstable dynamics of maglev systems pose significant challenges in designing effective controllers that ensure precise position tracking while countering external disturbances and model uncertainties. Various control strategies have been developed to address these challenges, including sliding mode control (SMC) [3], [4], adaptive control [3], [5], H-infinity control [6], and PID-based techniques [7]– [9]. Among these, SMC is widely recognized for its robustness against matched uncertainties and disturbances, making it a strong candidate for maglev control. However, traditional SMC struggles with chattering, a high-frequency oscillation that can introduce vibrations and degrade performance. Additionally, conventional modelbased controllers require precise system dynamics, which are often unavailable in real-world applications due to parameter variations, external influences, or environmental factors.

To mitigate chattering, higher-order sliding mode (HOSM) control has been proposed, which extends conventional SMC principles while significantly reducing oscillations. However, HOSM control alone still depends on accurate model parameters, making its effectiveness limited when system dynamics change. Parameter uncertainties can lead to slow responses, overshoot, and instability, requiring additional compensation techniques. In response, machine learning-based estimators such as radial basis function neural networks (RBFNNs) have been explored to enhance

[1] [1]Dept. of Electrical Engineering, Indian Institute of Technology, Patna, India, 801106 (email: brajesh_1821ee02@iitp.ac.in, yatendra@iitp.ac.in)
[2]Dept. of Electrical and Electronics Engineering, Birla Institute of Technology Mesra, Ranchi, India, 835215 (email: subratkumarswain@bitmesra.ac.in)

system robustness. While these approaches offer adaptability, they require extensive training, high computational effort, and may struggle with real-time implementation in highly nonlinear maglev systems. To tackle this challenge, several approaches have been introduced, such as non-singular terminal sliding mode control (NT-SMC) [10] and higher-order sliding mode (HOSM) [11]. These methods not only significantly reduce chattering effects but also ensure rapid compensation for system perturbations within a finite time.

To enhance robustness and real-time adaptability, this work integrates disturbance observer-Based control (DOBC) [12], [13] with higher-order sliding mode (HOSM) control, offering significant advantages over conventional estimators [14]. Unlike machine learning-based approaches such as radial basis function neural networks (RBFNNs) [15], [16], which require extensive training and large datasets, DOBC dynamically estimates disturbances in real-time without an offline learning phase. It provides immediate compensation for system uncertainties, ensuring consistent tracking performance even under unknown parameter variations. Compared to RBFNNs [17] and other model-based estimators, DOBC exhibits lower computational complexity [18], making it more suitable for real-time maglev control. Additionally, while conventional estimators primarily rely on model predictions, DOBC actively compensates for both matched and unmatched disturbances, significantly enhancing system stability and robustness. This paper aims to address the following critical challenges in maglev system control:

- Traditional SMC exhibits undesired high-frequency oscillations; HOSM control is employed to mitigate this issue. • Variations in system parameters degrade controller performance; DOBC enhances adaptability by providing realtime parameter correction.
- Environmental perturbations affect levitation stability; DOBC effectively attenuates disturbances, improving robustness.
- Many advanced controllers struggle with computational efficiency; the proposed DOBC-HOSM framework ensures fast, practical implementation.

The main contributions of this study are outlined as follows:

- Development of a nonlinear maglev system model using linear approximation and design of a HOSM controller based on reaching law formulation and stability analysis.
- Integration of DOBC with HOSM control to improve disturbance rejection and model parameter adaptation. This approach achieves robust position tracking with reduced chattering and enhanced disturbance attenuation. Finally, the Lyapunov function candidate proves the control approach's boundary and convergence.
- Comprehensive simulation-based validation in MATLAB, demonstrating that the proposed DOBC-HOSM controller outperforms conventional integer-order PID (IOPID) and standalone HOSM control in handling model uncertainties and external disturbances.

The outline of the paper is as follows: The details of the maglev system's model dynamics are explained in Section 2, focusing on the factors influencing the steel ball's position. Section 3 presents the proposed DOBC-based HOSM control strategy, which integrates a disturbance observer-based (DOB) approach to mitigate the effects of model parameter uncertainties and external disturbances, ensuring improved position control. Section 4 analyzes the simulation results, demonstrating the effectiveness of the proposed controller in comparison to traditional integer-order proportional-integralderivative (IOPID) and HOSM control methods. Finally, Section 5 concludes the paper.

2. MATHEMATICAL MODEL OF THE MAGNETIC LEVITATION SYSTEM

Fig. 1 presents a schematic representation of a magnetic levitation (maglev) system, specifically model 33-210 from Feedback Instruments Ltd. [19]. This diagram provides a conceptual overview of a practical maglev system commonly used in applications such as high-speed trains, magnetic bearings, and various industrial processes. The system under study consists of a steel ball that remains suspended within a voltage controlled magnetic field. The primary components include a ferromagnetic core coil, functioning as an actuator, and a position sensor that continuously

tracks the ball's displacement relative to the coil. The ball exhibits a single degree of freedom, constrained to vertical motion, which simplifies control implementation. The control system is computer-driven, with the controller designed and executed within MATLAB's simulink environment. The feedback loop is established through an infrared (IR) sensor, which detects the ball's position and transmits real-time data to the Simulink model via the PCI A/D-D/A interface card from advantech technologies.

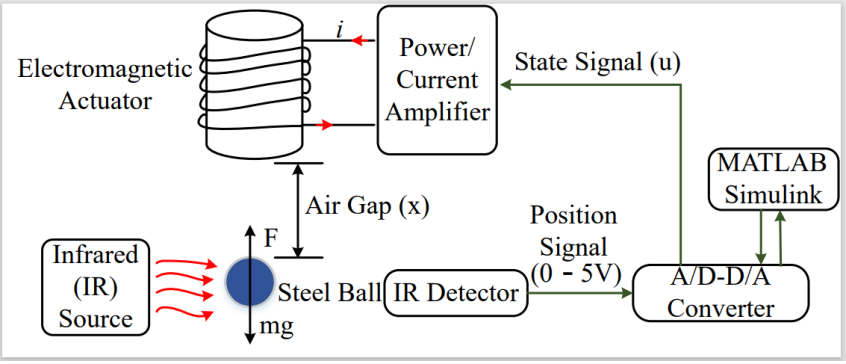

Fig.1. Schematic diagram of Maglev ball system.

The processed control signals are then conveyed to the physical system through an analog control interface board, which facilitates bidirectional communication between the computational and physical domains. This interface board, featuring analog-todigital and digital-to-analog converters, enables smooth and efficient signal transmission. The resulting control signal is applied to a current amplifier, which modulates the magnetic field intensity, thereby stabilizing the levitation of the steel ball and ensuring precise tracking of the desired reference trajectory.

To improve resilience of the system against uncertainties and external perturbations, a disturbance observer-based control (DOBC) approach is combined with a higher-order sliding mode (HOSM) controller. The fundamental nonlinear maglev model [3], formulated in terms of the ball's position x and the coil current i, is given by:

$$\begin{Bmatrix} m\frac{d^2x}{dt^2} = mg + F_{em}(i,x) \\ F_{em}(i,x) = -k\left(\frac{i}{x}\right)^2 \end{Bmatrix} \quad (1)$$

where m represents the mass of the steel ball, i denotes the coil current, x corresponds to the ball's position, and k is a constant dependent on the coil parameters. The gravitational acceleration is denoted by g, while the electromagnetic force acting on the ball is expressed as $F_{em}(i,x)$. Due to the inherent nonlinearity of the system dynamics, linearization is carried out around the equilibrium point (i_0, x_0) to facilitate controller design and system analysis. At this equilibrium, assuming $\ddot{x} = 0$, the system simplifies, one obtains

$$k = mg\left(\frac{i_0}{x_0}\right)^2 \quad (2)$$

The linearization is performed by assuming $x = x_0 + \Delta x$ and $i = i_0 + \Delta i$ where Δi and Δx represent the small deviation from the nominal position of the steel ball$x_0$and the coil current i_0. Thus, the nonlinear maglev model (1) can be linearized to

$$\Delta\ddot{x} = -\left(\frac{\partial F_{em}(i,x)}{\partial i}|_{(i_0,x_0)}\,\Delta i + \frac{\partial F_{em}(i,x)}{\partial x}|_{(i_0,x_0)}\,\Delta x\right) \quad (3)$$

where, $F_{em_i} = \frac{\partial F_{em}(i,x)}{\partial i}|_{(i_0,x_0)} = -k\frac{2i_0}{2{x_0}^2}$

and $F_{em_x} = \frac{\partial F_{em}(i,x)}{\partial x}|_{(i_0,x_0)} = -k\frac{2{i_0}^2}{2{x_0}^3}$

The transfer function is derived by estimating the partial derivatives and subsequently applying the Laplace transform to (3) as

$$\frac{\Delta x}{\Delta i} = \frac{F_{em_i}}{s^2 - F_{em_x}} \tag{4}$$

To compensate for modeling uncertainties and disturbances $d(t)$, a disturbance observer (DO) is designed to estimate and counteract the unknown disturbances affecting the system. Since the physical system depicted in Fig. 1 includes an internal current control loop that ensures the coil current i remains proportional to the control input u that is $i = k_1 u$, where k_1 is proportionality constant, the corresponding linearized system is formulated as

$$\Delta\ddot{x} = a\Delta x + b\Delta u + d(t) \tag{5}$$

where, $a = -k\frac{2{i_0}^2}{2{x_0}^3}$ and $b = k\frac{2i_0}{2{x_0}^2}$

Incorporating a DOBC or DO framework, an extended state observer (ESO) is designed to estimate both the system's internal uncertainties and external disturbances. The DO compensates for these perturbations, ensuring the system's stability and improving tracking accuracy. The state-space representation of the maglev system with DOBC is

$$\begin{cases} \dot{x}_1 = x_2 \\ \dot{x}_2 = a_0 x_1 + b_0 u + f(t) + \hat{d}(t) \\ y = x_1 \end{cases} \tag{6}$$

where y is the output, a_0, b_0 represent the nominal value of system parameter a and b, respectively, $f(t) = (a - a_0)x_1 + (b - b_0)\Delta u$ designates to the unknown internal dynamics, and model parameter uncertainties, while $\hat{d}(t)$ represents the estimated disturbance using the ESO. The subsequent section introduces a DO-based HOSM controller that utilizes the disturbance estimates from the DO to enhance the robustness of the system and mitigate chattering effects while ensuring precise position tracking of the maglev system. The variations in parameters a and b introduce complexities in precisely modeling the highly nonlinear, time-varying, and inherently unstable maglev system. To address these issues, the following section presents the development of an HOSM controller incorporating disturbance observer and examines stability of the system.

3. DISTURBANCE OBSERVER-BASED HOSM CONTROLLER DESIGN

Fig. 2 presents the overall framework of the proposed DOBC-integrated HOSM controller, developed to achieve precise position tracking in the maglev system.

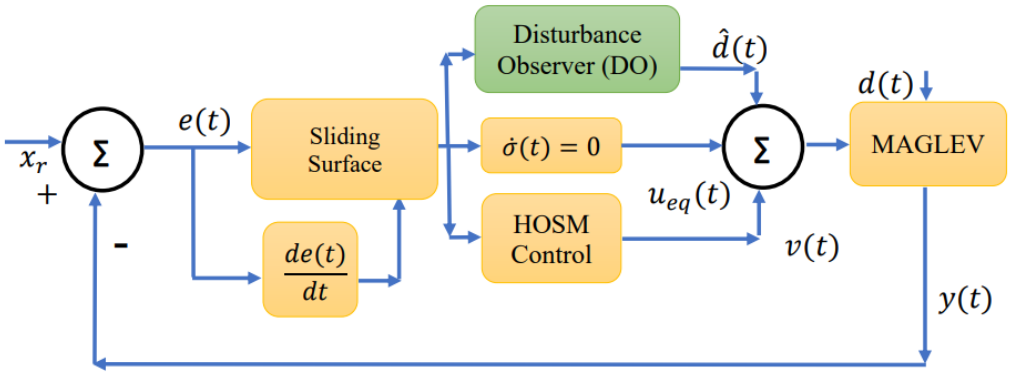

Fig.2. Proposed DOBC-based HOSM control for maglev ball.

3.1. Design of the HOSM Controller with Disturbance Observer

In this section, a HOSM controller combined with a disturbance observer (DO) is formulated to suppress chattering while effectively compensating for external disturbances. The tracking error dynamics are defined as

$$\begin{cases} e_1 = x_r - x_1 \\ \dot{e_1} = e_2 = \dot{x}_r - x_2 \end{cases} \quad (7)$$

where x_r represents the desired position and x_1 denotes the actual position of the steel ball. Under the influence of disturbances and parameter variations, the main goal is to drive the tracking error e_1 to zero within a finite time. Considering the system dynamics in (1), the sliding surface c is designed as

$$\sigma = e_2 + \lambda e_1 \quad (8)$$

where λ is the gain parameter designed, such as $\lambda > 0$. The final and optimal control output uf is ontained by combining the robust term $v(t)$from the HOSM controller and the estimated equivalent control input ueq. A Disturbance Observer (DO) is employed to estimate the disturbance term $d(t)$, thereby improving robustness. Hence, referring to (1)-(8), one can derive

$$\dot{\sigma} = \ddot{x}_r - \dot{x}_2 + \lambda(\dot{x}_r - \dot{x}_1) = -f(t) - a_0 x_1 - b_0 u - \hat{d}(t) + \ddot{x}_r + \lambda \dot{e}_1 \quad (9)$$

where, $\hat{d}(t)$ represents the estimated disturbance obtained from the DO. The equivalent control component is then derived as equating $\dot{\sigma} = 0$

$$u_{eq} = \frac{1}{b_0}(-f(t) - a_0 x_1 - \hat{d}(t) + \ddot{x}_r + \lambda \dot{e}_1) \quad (10)$$

To ensure error convergence in the presence of disturbances, the control input is designed as

$$u_f = \frac{1}{b_0}(-f(t) - a_0 x_1 - v(t) - \hat{d}(t) + \ddot{x}_r + \lambda \dot{e}_1) \quad (11)$$

where, $v(t)$ represents the robust term, expressed as [20]

$$\begin{cases} v(t) = -\eta_1 |\sigma(x,t)|^{1/2} sgn\big(\sigma(x,t)\big) + v_1(t)\_v_2(t) \\ v_1(t) = -\eta_2 sgn\big(\sigma(x,t)\big) \\ v_2(t) = -\eta_3 |\sigma(x,t)| \end{cases} \quad (12)$$

where $sgn\big(\sigma(x,t)\big)$ is the switching function defined as

$$sgn\big(\sigma(x,t)\big) = \begin{cases} 1 & \sigma > 0 \\ 0 & \sigma = 0 \\ -1 & \sigma < 0 \end{cases} \quad (13)$$

where, η_1, η_2, and η_3 are the robust gains that need to be appropriately tuned. A Lyapunov function candidate V is defined as

$$V = \frac{1}{2}\sigma^2 \quad (14)$$

From (8) - (12), it follows that

$$\dot{V} = \sigma\dot{\sigma} = \sigma(v(t) - d(t)) \quad (15)$$

For $\dot{V} < 0$, $||v(t)|| \geq \max(d(t))$ with $||d(t)|| \leq D$, where D indicates the maximum disturbance magnitude. The robust gains $\eta_1, \eta_2, \eta_3 > 0$, ensure stability for both $\sigma > 0$ and $\sigma < 0$. The disturbance observer estimates unknown

disturbances, leading to enhanced robustness compared to a traditional HOSM controller. This integration significantly improves tracking performance in the presence of model uncertainties and external perturbations.

3.2. Disturbance Observer-Based Compensation in HOSM Control

To enhance the robustness of the HOSM controller against disturbances, a DOBC scheme is integrated. The primary objective of DOBC is to estimate and compensate for disturbances in real time, thereby mitigating their adverse effects on system performance. The control strategy consists of three components: the equivalent control, robust control and the disturbance compensation term. The sliding variable is defined as:

$$\sigma = Ce \tag{16}$$

where C is a predefined vector ensuring that the sliding surface meets the desired system dynamics and $e = [e_1, e_2]$. The control law for the HOSM controller with disturbance compensation is expressed as:

$$u(t) = u_{eq}(t) + v(t) + u_{dobc}(t) \tag{17}$$

where $u_{eq}(t)$ represents the equivalent control and $u_{dobc}(t)$ denotes the disturbance compensation term. To estimate disturbances, a disturbance observer (DO) is formulated as:

$$\frac{d(\hat{d}(t))}{dt} = -l(\hat{d}(t) - \sigma) \tag{18}$$

where c is the estimated disturbance and $l > 0$ is the observer gain ensuring convergence. The disturbance compensation term is then given by

$$u_{dobc}(t) = -\hat{d}(t) \tag{19}$$

which counteracts the effects of the external disturbances. To analyze stability, consider the Lyapunov function candidate:

$$V = \frac{1}{2}\sigma^2 + \frac{1}{2\gamma}\tilde{d}^2 \tag{20}$$

where $\tilde{d}(t) = \hat{d}(t) - d(t)$ represents the estimation error and $\gamma > 0$ is a positive constant. Differentiating V and referring (10), (11) and (12), and $\dot{d}(t)$ yields

$$\begin{aligned} V &= \sigma\dot{\sigma} + \frac{1}{\gamma}\tilde{d}\frac{d(\tilde{c})}{dt} \\ &= \sigma\left(-f(t) - a_0 x_1 - v(t) - \hat{d}(t) + \ddot{x}_r + \lambda\dot{e}_1\right) + \frac{1}{\gamma}\tilde{d}\left(\frac{d(\hat{d})}{dt} - \dot{d}\right) \\ &= \sigma[\lambda\dot{e}_1 - v(t) + \frac{l\tilde{d}}{\gamma}\left(1 - \frac{\hat{d}}{\sigma}\right)] \end{aligned} \tag{21}$$

when $\sigma \neq 0$,

$$\begin{aligned} &\lambda\dot{e}_1 - v(t) + \frac{l\tilde{d}}{\gamma}\left(1 - \frac{\hat{d}}{\sigma}\right) \leq 0 \\ &||v(t)|| > \lambda\dot{e}_1 - v(t) + \frac{l\tilde{d}}{\gamma}\left(1 - \frac{\hat{d}}{\sigma}\right) \end{aligned} \tag{22}$$

where $||\tilde{d}|| < D$ and D represents the maximum disturbance estimation error. The satisfaction of (22) ensures that the condition $\dot{V} < 0$ is satisfied thereby ensuring asymptotic stability. The physical or comprehensive specifications of a magnetic levitation system are taken from [7].

TABLE I
Comparison of transient responses for various control strategies in position tracking (Fig. 7)

Transient Performance	IOPID	HOSM	DOB+HOSM
Overshoot (%)	72	22	0
Settling Time (sec)	2.2	0.35	0.2

4. RESULTS AND DISCUSSION

he effectiveness of the proposed DOBC-based HOSM control strategy has been evaluated through numerical simulations performed in MATLAB/Simulink. The primary objective of these simulations is to compare the performance of integerorder PID (IOPID), higher-order sliding mode (HOSM), and DOB-HOSM controllers in regulating the position of the maglev steel ball. By analyzing their transient and steady-state responses, the study aims to establish the superiority of the proposed DOB+HOSM approach.

Table I provides a comparative analysis of percentage overshoot and settling time across the three controllers. These indices are particularly significant as they inherently capture other dynamic parameters such as peak time, delay time, rise time, and overall error characteristics. To further evaluate robustness against model uncertainties, unknown dynamic parameters are introduced into the simulation, where $a_0 = 2180$ and $b_0 = -3518.85$ represent the system's uncertain dynamics.

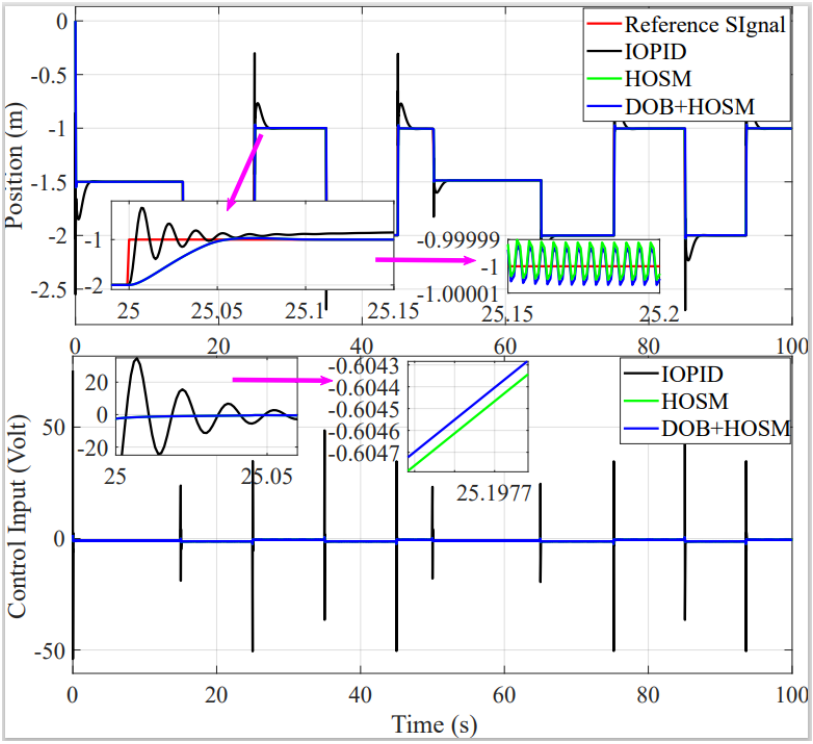

Fig.3. Performance evaluation of controller for square wave reference.

The simulation results in Fig. 3 illustrate the position tracking performance of all three controllers. While each method demonstrates rapid convergence to the reference trajectory, the DOB+HOSM controller exhibits superior tracking precision and dynamic response compared to the HOSM and IOPID controllers. The enhanced robustness of the proposed method is evident in its ability to achieve minimal steady-state error and faster stabilization. To assess the resilience of the controller against external disturbances, the Magnetic Levitation System (MLS) is subjected to sinusoidal and sawtooth wave perturbations. The disturbance amplitude is set to 10% of the reference trajectory's

mean value to simulate realistic external uncertainties. The output response and control signals under these disturbances are depicted in Figs. 4-5. A closer inspection of the results indicates that the DOBC-based HOSM controller exhibits significantly improved disturbance rejection compared to both the HOSM and IOPID controllers. The proposed control strategy successfully mitigates the effects of matched and unmatched disturbances, ensuring stable levitation even under fluctuating external conditions.

The robustness of the proposed controller is further vali1dated by evaluating its performance under parameter variations. The controller gains k1 and k2 are varied within a range of ±20% to analyze the impact of modeling uncertainties. As illustrated in Figs. 6-7, the DOBC+HOSM controller maintains stable and optimal control performance, whereas the HOSM and IOPID controllers exhibit noticeable deviations. In addition, the control voltage response in Figs. 3-5 highlights a key advantage of the proposed method—reduced overshoot and smoother control action. While the HOSM controller shows fluctuations when sensor gain k1 varies, the DOBC+HOSM controller generates a more stable and consistent control response, as depicted in Fig. 7. This reinforces the robustness and adaptability of the proposed method under sensor gain variations, further justifying its effectiveness over conventional approaches.

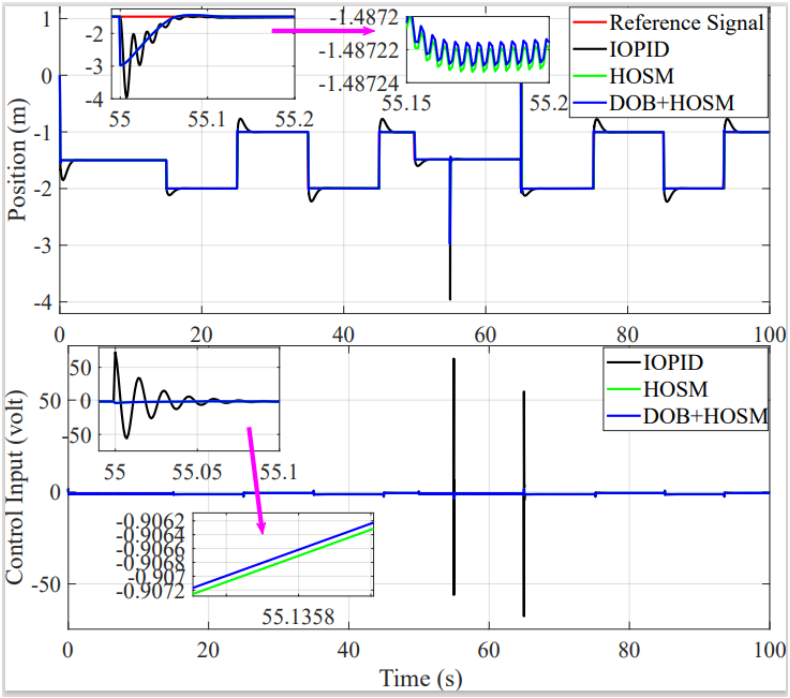

Fig.4. Performance evaluation of controller for sine wave disturbance.

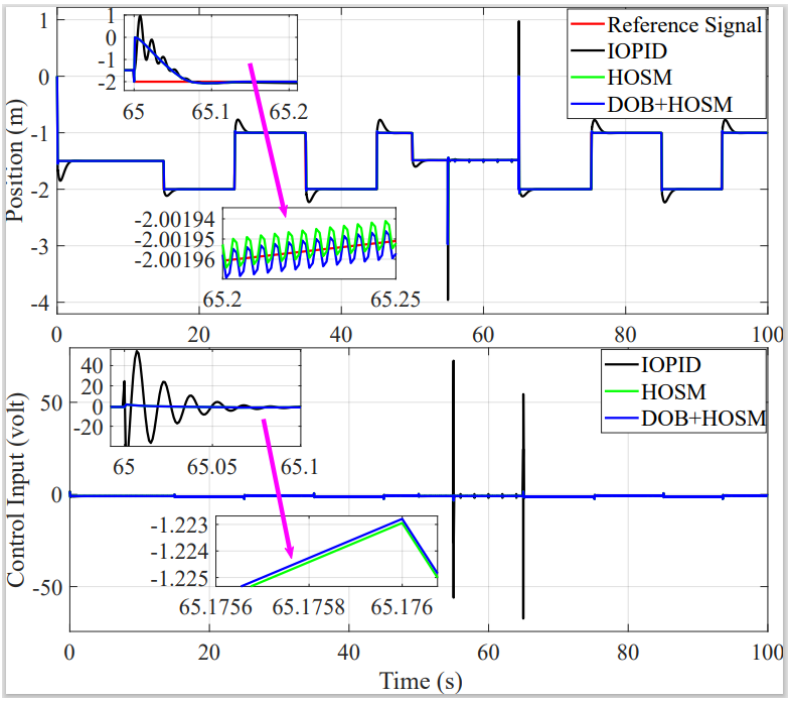

Fig.5. Performance evaluation of controller for sawtooth wave disturbance

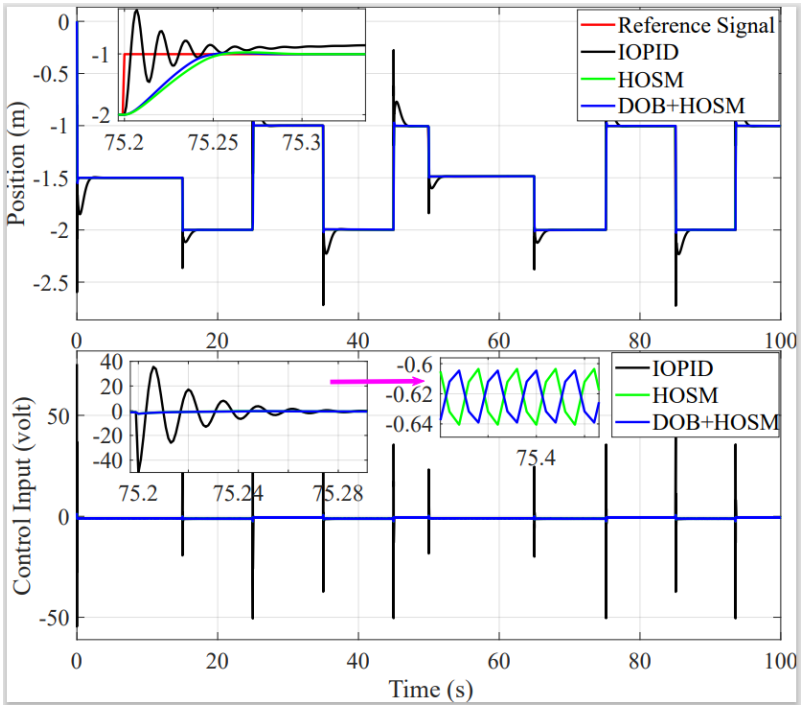

Fig. 6. Robust Performance evaluation of controller with $+20\%$ variation in the gains $k1$ and $k2$.

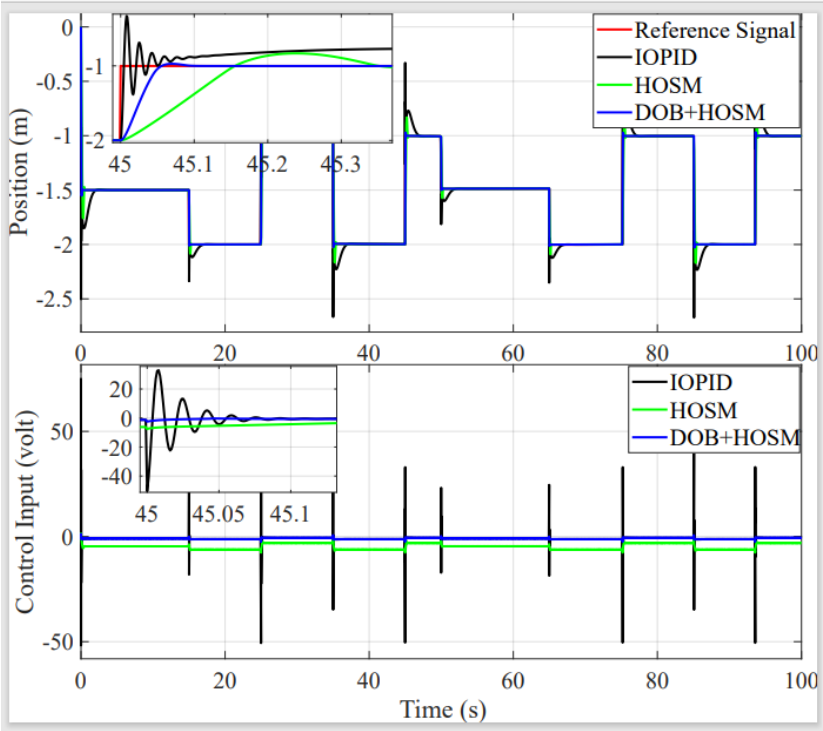

Fig. 7. Robust Performance evaluation of controller with -20% variation in the gains $k1$ and $k2$.

5. CONCLUSION

The effectiveness of the proposed disturbance observerbased control (DOBC) integrated with the higher-order sliding mode (HOSM) controller in mitigating disturbances and handling model parameter variations has been rigorously demonstrated in this study. The controller ensures stable levitation of the maglev system despite external perturbations and variations in system parameters, exhibiting enhanced robustness and rapid convergence. The proposed approach successfully mitigates model uncertainties while achieving precise position tracking, even in the presence of significant exogenous disturbances. Furthermore, the methodologies employed in this framework can be extended to other nonlinear systems, facilitating an in-depth investigation of their closed-loop behavior under various model uncertainties and nonlinear conditions. This adaptability highlights the potential of the DOBC-based HOSM controller in improving the performance of a wide range of nonlinear control applications.

REFERENCES

[1] M. Morishita, T. Azukizawa, S. Kanda, N. Tamura, and T. Yokoyama, “A new maglev system for magnetically levitated carrier system,” IEEE Transactions on Vehicular technology, vol. 38, no. 4, pp. 230–236, 1989.

[2] I. Boldea, L. N. Tutelea, W. Xu, and M. Pucci, “Linear electric machines, drives, and maglevs: An overview,” IEEE Transactions on Industrial Electronics, vol. 65, no. 9, pp. 7504–7515, 2017. [3] B. Kumar, S. K. Swain, S. Ghosh, S. K. Mishra, and Y. K. Singh, “Radial basis function-based adaptive gain super-twisting controller for magnetic levitation system with time-varying external disturbance,” IEEE Transactions on Transportation Electrification, vol. 10, no. 4, pp. 9121–9132, 2024.

[4] L. Yipeng, L. Jie, Z. Fengge, and Z. Ming, “Fuzzy sliding mode control of magnetic levitation system of controllable excitation linear synchronous motor,” IEEE Transactions on Industry Applications, vol. 56, no. 5, pp. 5585–5592, 2020.

[5] Z.-J. Yang and M. Tateishi, “Adaptive robust nonlinear control of a magnetic levitation system,” Automatica, vol. 37, no. 7, pp. 1125–1131, 2001.

[6] X. Wei and L. Guo, “Composite disturbance-observer-based control and h control for complex continuous models,” International Journal of Robust and Nonlinear Control: IFAC-Affiliated Journal, vol. 20, no. 1, pp. 106–118, 2010.

[7] S. K. Swain, D. Sain, S. K. Mishra, and S. Ghosh, “Real time implementation of fractional order pid controllers for a magnetic levitation plant,” AEU-International Journal of Electronics and Communications, vol. 78, pp. 141–156, 2017.

[8] R.-J. Wai, J.-D. Lee, and K.-L. Chuang, “Real-time pid control strategy for maglev transportation system via particle swarm optimization,” IEEE Transactions on Industrial Electronics, vol. 58, no. 2, pp. 629–646, 2010.

[9] B. Kumar, S. K. Swain, and N. Neogi, “Controller design for closed loop speed control of bldc motor,” International Journal on Electrical Engineering and Informatics, vol. 9, no. 1, p. 146, 2017.

[10] Y. Feng, X. Yu, and Z. Man, “Non-singular terminal sliding mode control of rigid manipulators,” Automatica, vol. 38, no. 12, pp. 2159–2167, 2002.

[11] M. K. Sarkar, A. Dev, P. Asthana, and D. Narzary, “Chattering free robust adaptive integral higher order sliding mode control for load frequency problems in multi-area power systems,” IET Control Theory & Applications, vol. 12, no. 9, pp. 1216–1227, 2018.

[12] K.-S. Kim, K.-H. Rew, and S. Kim, “Disturbance observer for estimating higher order disturbances in time series expansion,” IEEE Transactions on automatic control, vol. 55, no. 8, pp. 1905–1911, 2010.

[13] W.-H. Chen, J. Yang, L. Guo, and S. Li, “Disturbance-observer-based control and related methods—an overview,” IEEE Transactions on industrial electronics, vol. 63, no. 2, pp. 1083–1095, 2015.

[14] A. Mohammadi, M. Tavakoli, H. J. Marquez, and F. Hashemzadeh, “Nonlinear disturbance observer design for robotic manipulators,” Control Engineering Practice, vol. 21, no. 3, pp. 253–267, 2013.

[15] X. Chen, W. Shen, M. Dai, Z. Cao, J. Jin, and A. Kapoor, “Robust adaptive sliding-mode observer using rbf neural network for lithium-ion battery state of charge estimation in electric vehicles,” IEEE Transactions on Vehicular Technology, vol. 65, no. 4, pp. 1936–1947, 2015.

[16] Z. Chen, Y. Zhang, Y. Nie, J. Tang, and S. Zhu, “Adaptive sliding mode control design for nonlinear unmanned surface vessel using rbfnn and disturbance-observer,” Ieee Access, vol. 8, pp. 45 457–45 467, 2020.

[17] B. Kumar, S. K. Swain, S. K. Mishra, and Y. K. Singh, “Artificial neural network-based sliding mode position tracking control for maglev system,” in 2023 IEEE 3rd International Conference on Smart Technologies for Power, Energy and Control (STPEC). IEEE, 2023, pp. 1–6.

[18] W.-H. Chen, “Disturbance observer-based control for nonlinear systems,” IEEE/ASME transactions on mechatronics, vol. 9, no. 4, pp. 706–710, 2004.

[19] M. Levitation, “Control experiments feedback instruments limited,” 2011.

[20] J. J. Rath, K. C. Veluvolu, M. Defoort, and Y. C. Soh, “Higher-order sliding mode observer for estimation of tyre friction in ground vehicles,” IET Control Theory & Applications, vol. 8, no. 6, pp. 399–408, 2014.